Progress In Electromagnetics Research M, Vol. 120, 29–40, 2023

An Multilayer Metamaterial Inspired Antenna for In-Body and On-Body Application

Siddhant Goswami[1, *], Deepak C. Karia[1], Tapas Bhuiya[2], and Vikalp Singh[2]

Abstract—In this research work, a flexible metamaterial inspired antenna is proposed. The substrate is made of polyamide making it bendable. The stepwise detail analysis is discussed, and the antenna has two complimentary split resonators with circular ring placed in the ground plane. A superstrate along with an EBG structure is added in the final design. Mathematical modelling is done to prove metamaterial structure. To test the on-body results, first the permittivity of different fabrics is measured using DSL-01 (SES Instruments Pvt. Ltd). Phantom solution is required to test In-Body (Implantable) results.

1. INTRODUCTION

There has been rapid growth seen in the area of wireless communication. In the medical communication system, antenna is the main element responsible for transmission and reception of signals. In medical technology, it is mainly used in medical implants [1–3], microwave imaging, capsule endoscopy [4, 5], hyperthermia treatments, microwave breast cancer detection system [6, 7], and wireless monitoring. Minimizing the size with better performance has been the primary objective of recent researcher trends. Researchers have come to note that flexible antennas are better than rigid antennas which sometimes create uncomfortable feeling when being placed on human hand [8–10]. As compared with the conventional antenna, metamaterial helps to decrease the size, with an improved performance. Due to optimal size, metamaterial has wide growth in medical applications [11–13].

Literature shows significant size reduction techniques using metamaterial split ring resonator (SRR), complementary triangular ring resonator, complementary split ring resonator, adding slots to patch, using C-shaped slot, triangular electromagnetic and complementary triangular electromagnetic resonator [14, 15].

Implantable Environment: To test antenna in implantable environment, designing phantom solution is a great challenge. The effect of phantom on antenna parameters should be minimum. Researchers have taken several efforts for phantom such as making human muscle mimicking fluid, Fat, and cancer phantom [16].

Wearable Environment: Flexible antennas play a major role in wireless body area network [17]. The effect of different cloths on antenna parameters should be minimum when antenna is tested in a wearable environment. In the current research work, permittivity values of different cloths are tested on DSL-01 (SES Instruments Pvt. Ltd).

2. CHALLENGES INVOLVED

- To study when antenna comes in contact with human body, the performance of the antenna degrades. This body effect should be reduced.
- To study comparative analysis between on-body and in-body testing is difficult.

Received 27 May 2023, Accepted 27 September 2023, Scheduled 16 October 2023
* Corresponding author: Siddhant Goswami (siddhantgoswami23@gmail.com).
[1] Sardar Patel Institute of Technology, Mumbai, India. [2] SAMEER IIT Bombay, India.

3. ANTENNA DESIGN METHODOLOGY

There are two steps designed to get final result. The antenna has also been tested in the vicinity of different fabrics and in implantable environment. The design model is shown in Fig. 1(a) and Fig. 1(b).

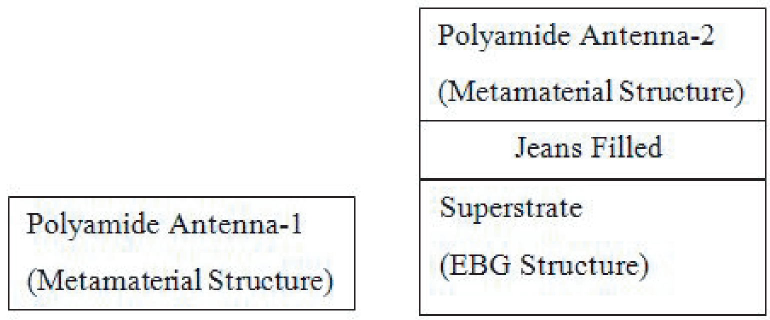

(a) (b)

Figure 1. (a) Step -1 (Model-1). (b) Step-2 (Model-2).

4. STEPWISE DESIGN ANALYSIS

Several trails are made to optimize antenna design.

4.1. Step 1 (Antenna-I)

In this step, antenna has two complimentary split resonators with a circular ring placed in the ground plane. The prepared top view and bottom view of the HFSS model are depicted in Fig. 2(a) and Fig. 2(b). The thickness of the antenna substrate is 0.3 mm with polyamide material. The fabricated antenna is shown in Fig. 3(a) and Fig. 3(b). Fig. 5(a) depicts the simulated and measured return losses for Antenna-I. Fig. 4(a) depicts the return loss without metamaterial complementary split-ring resonator

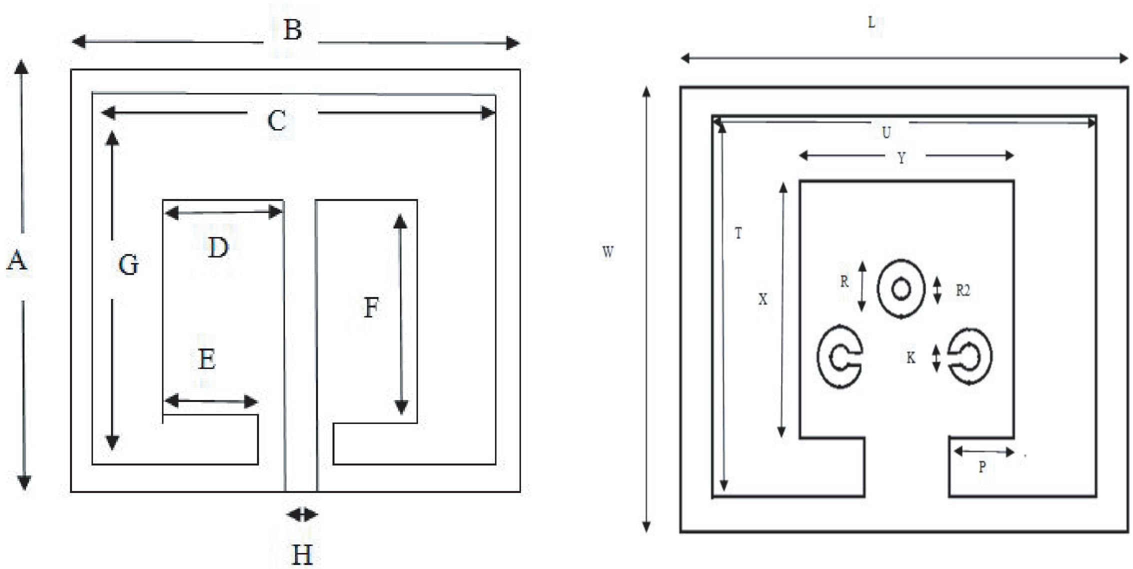

(a) (b)

Figure 2. Step 1: (a) HFSS design model top view, (b) HFSS design model bottom view.

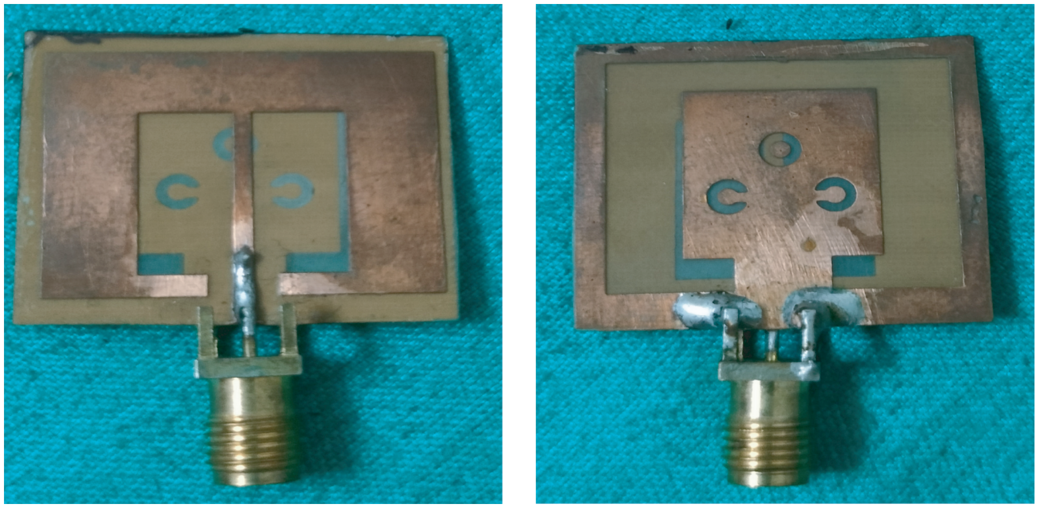

(a) (b)

Figure 3. Step 1: (a) Fabricated top view, (b) fabricated bottom view.

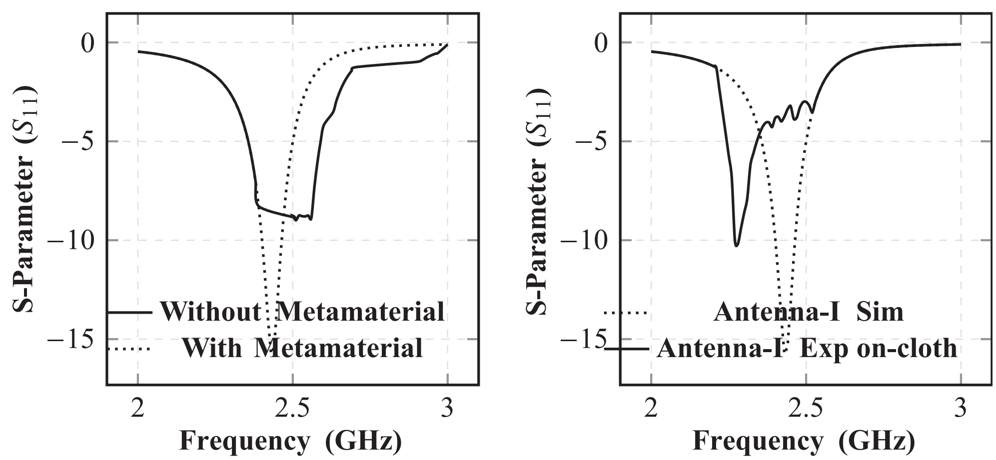

(a) (b)

Figure 4. (a) Antenna-I — Without metamaterial and with metamaterial. (b) Measured return loss of Antenna-I on cloth material.

(CSRR) and with metamaterial CSRR in ground plane. Fig. 4(b) depicts the return loss of Antenna-I when it is placed in free space and on cloth material. Antenna-I shows depreciated value in return loss when being placed in contact of different cloths. Antenna-II shows minimum effect of surrounding textile material on return loss due to the use of superstrate (Minimizing the cloth effect). The simulated return loss for Antenna-I is −15.75 dB at 2.43 GHz, and measured return loss is −23.75 dB at 2.33 GHz. The radiation pattern of Antenna-I is shown in Fig. 6(a).

4.2. Step 2 (Antenna-II)

In this step, the designed antenna is the same as step 1, with an additional superstrate. The gap between substrate and superstrate is filled with jeans of thickness 1.6 mm. The superstrate bottom patch consists of a square electromagnetic band gap (EBG) structure. The top view of fabricated antenna is shown in Fig. 7(b), and the design is shown in Fig. 7(a). The bottom view of fabricated antenna is shown in

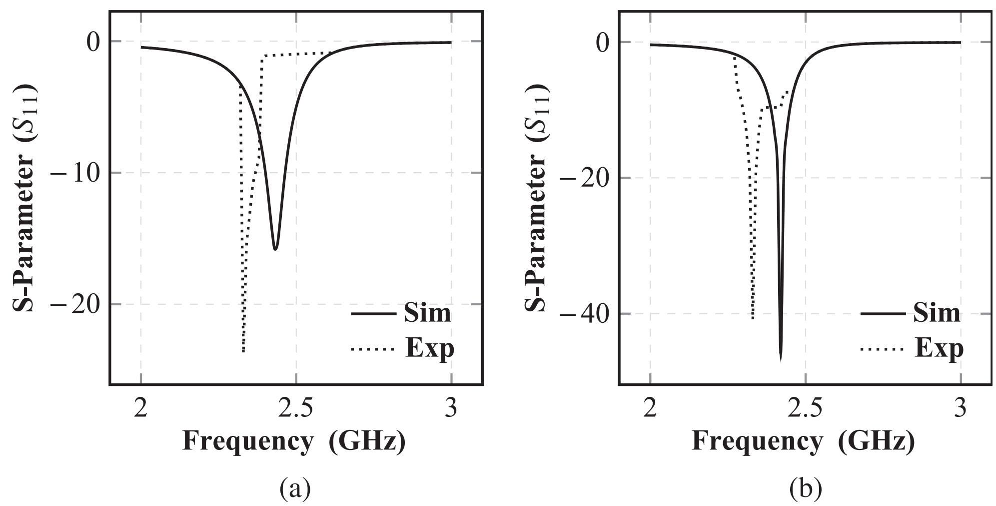

Figure 5. (a) Antenna-I — Experimental and simulated return loss. (b) Antenna-II — Experimental and simulated return loss.

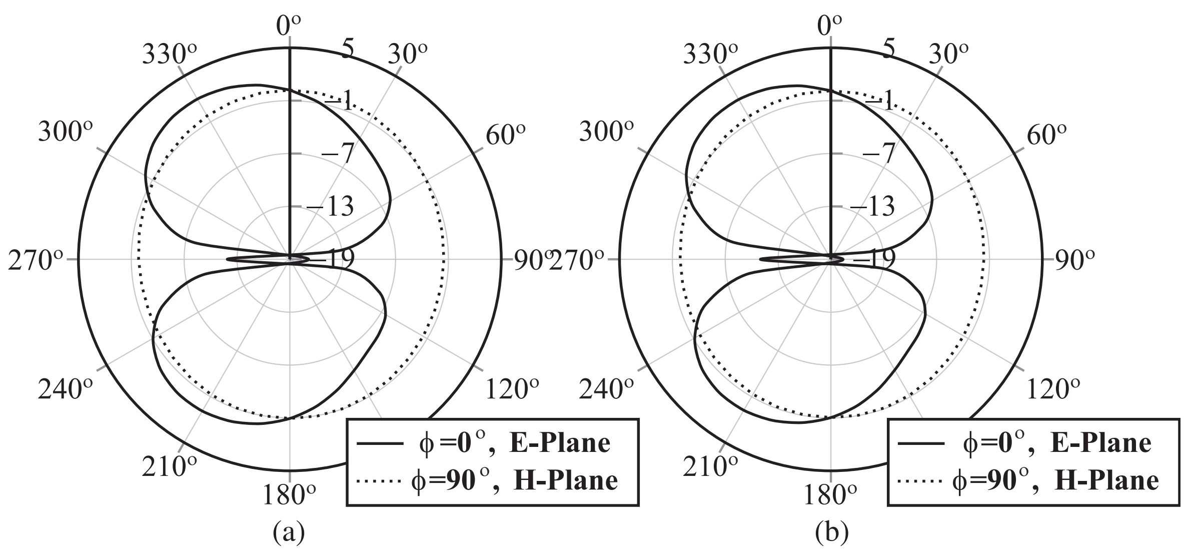

Figure 6. (a) Radiation pattern of Antenna-I. (b) Radiation pattern of Antenna-II.

Fig. 8(b), and the design is shown in Fig. 8(a).

The simulated and measured return losses for Antenna-II are shown in Fig. 5(b). The simulated return loss is −45 dB at 2.42 GHz, and measured return loss is −40 dB at 2.33 GHz. The radiation pattern of Antenna-II is shown in Fig. 6(b). The dimensions of Antenna-I and Antenna-II are shown in Table 1.

5. SPECIFIC ABSORPTION RATE

Watts per kilogram (W/kg) is the unit used to compute the specific absorption rate (SAR) value. A crucial factor in antenna design is SAR; it should be at the lower end to prevent any harmful effects on the human body. 1.6 Watts per kilogram is the maximum permitted SAR limit. The SAR value of Antenna-I is 1.3 W/kg, and that of Antenna-II is 1 W/kg obtained when input power is 1 watt as shown in Figure 9. The SAR value of Antenna-I is 0.7 W/kg, and Antenna-II is 0.3 W/kg obtained when input power is 100 milliwatt as shown in Figure 10. As compared with Antenna-I, Antenna-II has shown lower

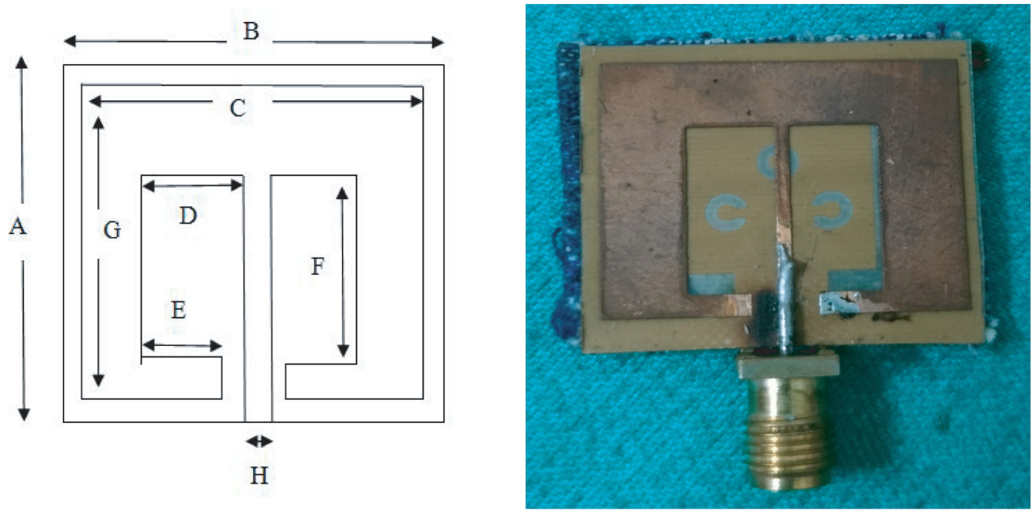

(a) (b)

Figure 7. Step 2: (a) HFSS design model top view, (b) top view of fabricated antenna.

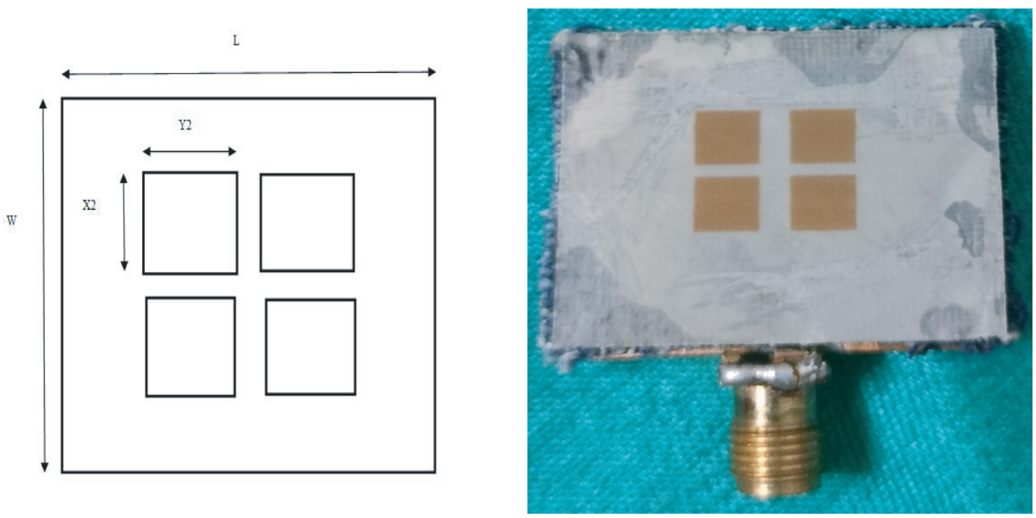

(a) (b)

Figure 8. Step 2: Textile gap coupled antenna. (a) HFSS design model EBG (Superstrate) — Bottom view, (b) bottom view of fabricated antenna (superstrate) .

SAR value due to the use of superstrate. To analyze the SAR value, a three layer human body model is used. The three layer model consists of skin, fat, and muscle. The properties of the three layer human model are shown in Table 2. While SAR is calculated, the gap between antenna and body model is 5 mm.

6. METAMATERIAL DESIGN PROOF

The given antenna consists of two split ring resonators (SRRs), along with a feeding transmission line (FTL) exhibiting metamaterial characteristics. The antenna has been designed on a polyamide substrate. The FTL is sketched on the opposite portion of the substrate. The excitation is supplied to the resonator through the FTL as shown in Fig. 9(a) and Fig. 9(b).

Table 1. Dimensions of Antenna-I and Antenna-II.

Parameters	Dimensions obtained	Parameters	Dimensions obtained
A	23 mm	L	27 mm
B	27 mm	W	23 mm
C	25 mm	U	23 mm
D	6 mm	T	19 mm
E	4 mm	X	13 mm
G	20 mm	Y	13 mm
F	13 mm	R	2.8 mm
H	0.6 mm	$R2$	1.5 mm
L	27 mm	K	0.8 mm
W	23 mm	P	3.4 mm
$X1$	4 mm	$X2$	4 mm

Table 2. Properties of three layer human model.

Layer	Thickness mm	ϵ_r
Skin	2	38
Fat	5	5.28
Muscle	20	52.7

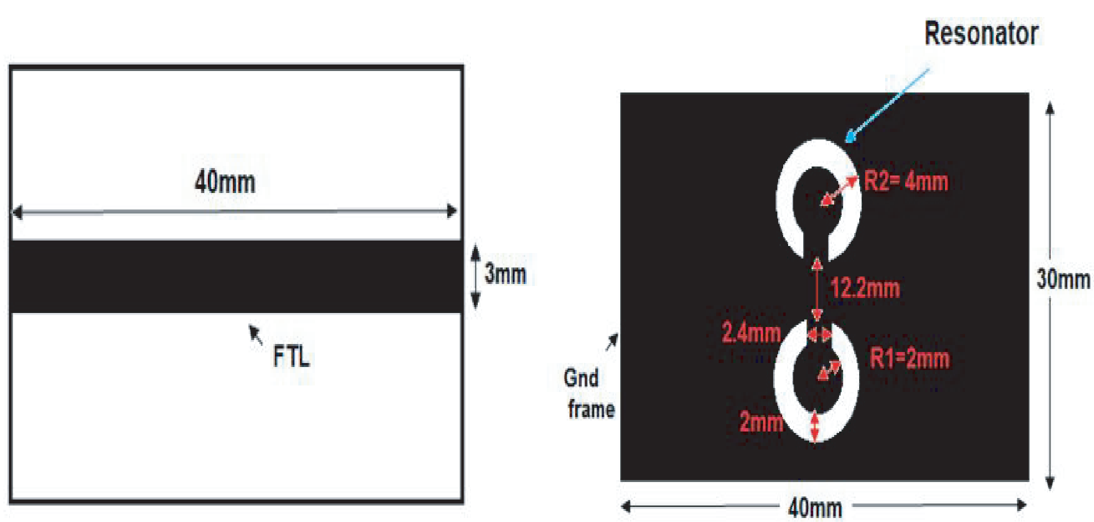

(a) (b)

Figure 9. (a) Antenna simulated antenna top view for metamaterial validation. (b) Antenna simulated antenna bottom view for metamaterial validation.

6.0.1. Characterization of Metamaterial

The Nicolson-Ross-Weir (NRW) method is used to characterize the metamaterial properties [18]. The values of the refractive index depend on the values of the permeability and permittivity. The NRW method is mathematically expressed with below equations.

$$X = ((S_{11})^2 + (S_{21})^2 + 1)2S_{11} \tag{1}$$

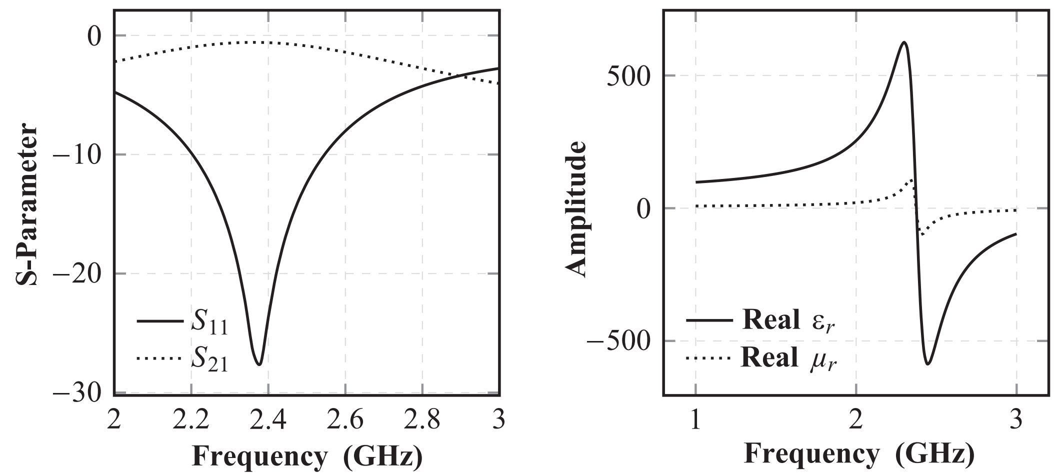

(a) (b)

Figure 10. (a) S-parameters — S_{11} and S_{21}. (b) Magnitude of effective parameters.

$$\tau = X \pm \sqrt{X^2 - 1} \tag{2}$$

The obtained X value can be substituted in (2) to get the value of τ from S_{11} and S_{21}.

$$T = \frac{S_{11} + S_{21} - \tau}{1 - \tau(S_{11} + S_{21})} \tag{3}$$

$$K = \log \frac{1}{|\tau|} + j\frac{2m\pi - phase(T)}{d} \quad m = 0, \pm 1, \pm 2 \tag{4}$$

The value of K can be calculated using Equations (3) and (2).

$$\epsilon = \frac{K}{K_0} * \frac{1 - \tau}{1 + \tau} \tag{5}$$

$$\mu = \frac{K}{K_0} * \frac{1 + \tau}{1 - \tau} \tag{6}$$

where μ denotes the permeability, ϵ the permittivity, and k_0 the propagation constant in free space. The values of μ and ϵ can be calculated using Equations (5) and (6).

The obtained scattering parameters S_{11} and S_{21} are shown in Fig. 10(a). The permittivity has negative regions of frequency from 2.18 to 2.66 (GHz), and permeability shows negative band from 2.10 to 2.72 (GHz) as shown in Fig. 10(b) and Table 3. Therefore, the proposed design depicted double-negative properties in the bandwidth from 2.1 GHz to 2.7 GHz, and all parameters had a negative peak at around frequency 2.4 GHz.

Table 3. Effective parameters negative index frequency region.

Sr. No.	Parameters	Negative index frequency region (GHz)
1	Permittivity (ϵ_r)	2.18–2.64
2	Permeability (μ_r)	2.10–2.72

7. CALCULATION OF PERMITTIVITY FOR DIFFERENT FABRICS (ON BODY)

The testing of permittivity for the fabrics is done for body area network. The test results for dielectric constant of different samples are shown below. They are tested on dielectric constant of solids and

(a) (b)

Figure 11. (a) Floor Cotton capacitance. (b) Curtain Cloth capacitance.

(a) (b)

Figure 12. (a) Pure Cotton capacitance. (b) Turkish Cloth capacitance.

liquids model: DSL-01 (SES Instruments Pvt. Ltd). Fig. 11(a) and Fig. 11(b) show measured floor cotton and curtain cloth capacitance. Fig. 12(a) and Fig. 12(b) show measured pure cotton and turkish cloth capacitance. Fig. 13(a) and Fig. 13(b) show measured polyster cotton and jeans cotton cloth capacitance. Table 4 shows the experimental permittivity obtained from variety of different fabrics.

The designed Antenna-II is tested on different fabrics such as Jeans as shown in Fig. 14(a) and curtain cloth as shown in Fig. 14(b). using Feildfox N9912A. The return loss obtained is about -32 dB. No major difference is observed after testing Antenna-II on different cloths. As compared with Antenna-I, Antenna-II has low effects of cloth on return loss parameter.

8. EXPERIMENTAL RESULTS FOR IN-BODY (IMPLANTABLE)

8.1. Practical Setup

The major components used for experiment are shown in Table 5.

(a) (b)

Figure 13. (a) Polyster capacitance. (b) Jeans Cotton capacitance.

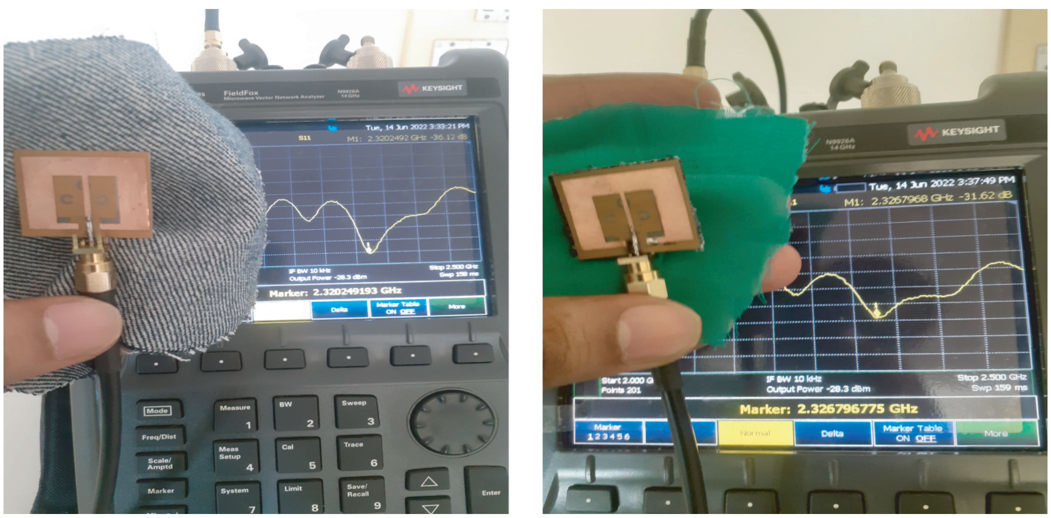

(a) (b)

Figure 14. (a) Return loss of Antenna-II on Jeans Fabric. (b) Return loss of Antenna-II Curtain Cloth.

Table 4. Permittivity of different fabrics.

Sample	**Thickness**	**Diameter**	**Capacitance at 25 C**	**Dielectric constant $K = (Cd)/(A\epsilon_0)$**
Floor Cotton	0.19×10^{-3} m	50 mm	150.25 pf	1.64
Curtain Cotton	0.21×10^{-3} m	50 mm	114.58 pf	1.38
Pure Cotton	0.23×10^{-3} m	50 mm	121.58 pf	1.61
Turkish	0.58×10^{-3} m	50 mm	56.66 pf	1.89
Polyster	0.16×10^{-3} m	50 mm	133.95 pf	1.23
Jeans Cotton	0.77×10^{-3} m	50 mm	70.94 pf	3.14

Table 5. Components used for calculating permittivity.

Name of component	Description
E5060A Vector Network Analyzer	E506A Vector Network Analyzer (5 Hz to 20 GHz) is used to measure return loss of antenna. We can also use Feildfox N9912A (30 kHz to 26.5 GHz) as an alternative
85070E dielectric probe kit	The 85070E dielectric probe kit is used to measure dielectric properties of liquid, internal calculation of software is dependent on Nicolson's Ross Method [19]. We can also use N1501A dielectric probe kit (range — 200 MHz to 50 GHz) as an alternative
Agilent Technology 85070E Software tool	This software is used to convert return loss obtained after dipping into liquid to the permittivity of liquid.
ECAL holder	used for calibrating VNA
Probe stand	The height of probe stand is 24 inches and base dimensions is 13 × 7 inches
50 Ω open ended coaxial probe	50 Ω cable is used for good impedance matching.

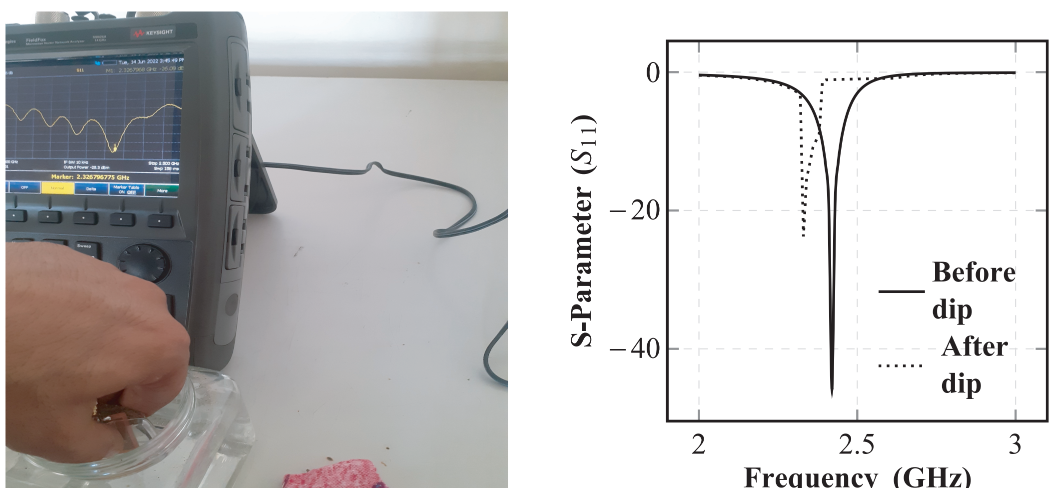

(a) (b)

Figure 15. (a) Experimental setup for measuring return loss of implantable antenna (Antenna-II) and calculating permittivity of liquid. (b) Comparison of return loss of antenna before and after dipping antenna in liquid.

The metamaterial-inspired antenna is submerged in a fluid that resembles muscle. The experimental setup for measuring return loss of implantable antenna is shown in Fig. 15(a). Initially, air bubbles would (not) travel at tip of probe, which should be avoided to have accurate results. The simulated return loss of metamaterial inspired antenna (Antenna-II) is about −45 dB at 2.42 GHz. After inserting antenna into fluid that resembles muscle, it is seen that the return loss decreases. The return loss changes to −26.0 dB at 2.33 GHz as shown in Fig. 15(b).

9. CONCLUSION

This work has discussed several methods for size reduction of antenna. The metamaterial inspired antenna is suitable to work for the wireless body area network environment (Both in body and on body). The simulated return loss is about −45 dB at 2.42 GHz, and measured return loss in free space is about −40 dB at 2.33 GHz.

This work also has been done for testing antenna on different fabrics. For every fabric such as Jeans, and floor cotton permittivity is calculated using DSL-01 (SES Instruments Pvt. Ltd). The effect of antenna placed on different fabrics is discussed.

As compared with Antenna-I, Antenna-II has shown better performance when being placed near textile material due to the use of a superstrate structure.

ACKNOWLEDGMENT

The authors would like to thank Mr. Tapas Bhuiya (SAMEER, IIT Bombay), Mr. Sunil Patankar, Applied science and humanity department for providing timely help and support.

REFERENCES

1. Kumar, S. A., T. Shanmuganantham, and G. Sasikala, "Design and development of implantable CPW fed monopole U slot antenna at 2.45 GHz ISM band for biomedical applications," *Microwave and Optical Technology Letters*, Vol. 57, No. 7, 1604–1608, 2015.
2. Liu, C., Y. X. Guo, R. Jegadeesan, and S. Xiao, "In vivo testing of circularly polarized implantable antennas in rats," *IEEE Antennas and Wireless Propagation Letters*, Vol. 14, 783–786, 2014.
3. Kiourti, A. and K. S. Nikita, "A review of implantable patch antennas for biomedical telemetry: Challenges and solutions [Wireless corner]," *IEEE Antennas and Propagation Magazine*, Vol. 54, No. 3, 210–228, 2012.
4. Shah, S. M. A., M. Zada, J. Nasir, O. Owais, A. Iqbal, and H. Yoo, "Miniaturized four-port MIMO implantable antenna for high data-rate wireless capsule endoscopy applications," *IEEE Transactions on Antennas and Propagation*, Vol. 71, No. 4, 3123–3133, 2023.
5. Wang, G. B., X. W. Xuan, D. L. Jiang, K. Li, and W. Wang, "A miniaturized implantable antenna sensor for wireless capsule endoscopy system," *AEU — International Journal of Electronics and Communications*, Vol. 143, 154022, 2022.
6. Li, Y., E. Porter, A. Santorelli, M. Popović, and M. Coates, "Microwave breast cancer detection via cost-sensitive ensemble classifiers: Phantom and patient investigation," *Biomedical Signal Processing and Control*, Vol. 31, 366–376, 2017.
7. Çalışkan, R., S. S. Gültekin, D. Uzer, and A. Dündar, "Microstrip patch antenna design for breast cancer detection," *Procedia — Social and Behavioral Sciences 2015, World Conference on Technology, Innovation and Entrepreneurship*, Vol. 195, 2905–2911, 2015.
8. Abbas, S. M., K. P. Esselle, and Y. Ranga, "An armband-wearable printed antenna with a full ground plane for body area networks," *2014 IEEE Antennas and Propagation Society International Symposium (APSURSI)*, Memphis, TN, USA, 2014.
9. Shrestha, S., M. Agarwal, P. Ghane, and K. Varahramyan, "Flexible microstrip antenna for skin contact application," *International Journal of Antennas and Propagation*, Vol. 2012, 2012.
10. Wang, M., Z. Yang, J. Wu, et al., "Investigation of SAR reduction using flexible antenna with metamaterial structure in wireless body area network," *IEEE Transactions on Antennas and Propagation*, Vol. 66, No. 6, 3076–3086, 2018.
11. Ali, T., A. M. Saadh, R. C. Biradar, J. Anguera, and A. Andújar, "A miniaturized metamaterial slot antenna for wireless applications," *AEU — International Journal of Electronics and Communications*, Vol. 82, 368–382, 2017.

12. Raval, F., Y. Kosta, and H. Joshi, "Reduced size patch antenna using complementary split ring resonator as defected ground plane," *AEU — International Journal of Electronics and Communications*, Vol. 69, No. 8, 1126–1133, 2015.
13. Virdee, B., *Grand Challenges in Metamaterial Antennas*, 2022.
14. Zhu, C., T. Li, K. Li, et al., "Electrically small metamaterial-inspired triband antenna with meta-mode," *IEEE Antennas and Wireless Propagation Letters*, Vol. 14, 1738–1741, 2015.
15. Bhattacharjee, S., S. Maity, S. R. B. Chaudhuri, and M. Mitra, "Metamaterial inspired wideband biocompatible antenna for implantable applications," *IET Microwaves, Antennas & Propagation*, Vol. 12, No. 11, 1799–1805, 2018.
16. Goswami, S. and D. C. Karia, "A metamaterial-inspired circularly polarized antenna for implantable applications," *Engineering Reports*, Vol. 2, No. 10, e12251, 2020.
17. Goswami, S. and D. C. Karia, "An metamaterial inspired antenna with CSRR and rectangular SRR based flexible antenna with jeans gap filled for wireless body area network," *Progress In Electromagnetics Research C*, Vol. 122, 165–181, 2022.
18. Mahmud, M., M. Islam, N. Misran, M. Singh, and K. Mat, "A negative index metamaterial to enhance the performance of miniaturized UWB antenna for microwave imaging applications," *Applied Sciences*, Vol. 7, No. 11, 1149, 2017.
19. Rothwell, E. J., J. L. Frasch, S. M. Ellison, P. Chahal, and R. O. Ouedraogo, "Analysis of the Nicolson-Ross-Weir method for characterizing the electromagnetic properties of engineered materials," *Progress In Electromagnetics Research*, Vol. 157, 31–47, 2016.